Phys. Status Solidi B **247**, No. 3, 469–475 (2010) / **DOI** 10.1002/pssb.200983081

physica status solidi b
www.pss-b.com
basic solid state physics

Ferromagnetic and ferroelectric quantum phase transitions

Stephen Rowley, Robert Smith, Mark Dean, Leszek Spalek, Michael Sutherland, Montu Saxena, Patricia Alireza, Chris Ko, Cheng Liu, Emma Pugh, Suchitra Sebastian, and Gilbert Lonzarich*

Cavendish Laboratory, University of Cambridge, JJ Thomson Avenue, Cambridge CB3 0HE, UK

Received 27 November 2009, accepted 4 December 2009
Published online 24 February 2010

PACS 71.10.Hf, 72.15.Eb, 72.80.Ga, 75.10.Lp, 75.20.Hr, 75.30.Kz, 77.80.–e

* Corresponding author: e-mail GGL1@cam.ac.uk, Phone: +44 (0)1223 337351, Fax: +44 (0)1223 768140

The applicability of mean field models of ferroelectric and ferromagnetic quantum critical points is examined for a selection of d-electron systems. Crucially, we find that the tendency of the effective interaction between critical fluctuation modes to become attractive and anomalous as the ordering temperatures tend to absolute zero results in particularly complex and striking phenomena. The multiplicity of quantum critical fields at the border of metallic ferromagnetism, in particular, is discussed here.

1 Introduction We consider the nature of quantum phase transitions driven by changes in composition of materials or changes in applied pressure, magnetic field or electric field in the low temperature limit. Quantum phase transitions exhibit surprisingly subtle and complex behaviour even in comparatively simple examples of cubic ferroelectric materials and ferromagnetic metals of high purity, which will be the main focus of this article.

Early descriptions of quantum critical points (QCP), developed independently in ferroelectric materials [1] and ferromagnetic metals [2–6] in the 1970s, were based essentially on ϕ^4-quantum field models. They differ from the Ginzburg-Landau-Wilson models of classical critical phenomena by the inclusion of the dynamics of the order parameter field $\phi(r,\tau)$, which represents a coarse-grained electric or magnetic polarization as a function of spatial coordinate r and temporal coordinate τ (the imaginary time, which has a finite range at non-zero temperatures, $0 < \tau < \hbar/k_BT$) [7]. The inclusion of the thermal coordinate increases the relevant dimension from the spatial dimension d to the effective dimension $d_{\text{eff}} = d + z$, where z is the dynamical exponent defining the dispersion relation, *i.e.*, the wavevector dependence of the frequency spectrum of fluctuations of the field ϕ at small wavevectors (see §2).

The self-consistent-field approximation, which applies in the case of classical critical phenomena for $d > 4$ in the classical ϕ^4 model, might apply under a less restrictive condition $d > 4 - z$ in the ϕ^4 quantum treatment of critical phenomena. However, as discussed below, there are other more subtle ways in which quantum and classical phase transitions can differ [8, 9].

We begin by considering properties of ferroelectric and ferromagnetic quantum phase transitions that seem capable of a description in the self-consistent-field approximation as outlined above. We then turn to examples of apparent breakdowns of this approximation and discuss the possible reasons for the unexpected behaviours observed.

2 Quantum criticality in a paraelectric material We first consider the transition from a ferroelectric state to a paraelectric state as a function of a 'quantum tuning' parameter such as pressure, chemical composition or isotopic composition [10]. In a displacive ferroelectric material characterized by a phase transition of 2nd order, the frequency gap, Δ, of an optical vibrational mode vanishes continuously along with the Curie temperature T_C at the QCP, in for instance a temperature-pressure phase diagram. At this critical point the dispersion relation of the optical mode becomes analogous to that of an acoustic mode with $z = 1$. In the self-consistent-field approximation to the quantum ϕ^4 model this implies that the electric susceptibility or dielectric function diverges as $1/T^2$ in the quantum critical regime (Table 1) [1, 11–14].

As shown in Fig. 1, this prediction is found to be consistent qualitatively and roughly quantitatively with observations in the cubic perovskite $SrTiO_3$ in the range 5

© 2010 WILEY-VCH Verlag GmbH & Co. KGaA, Weinheim

Table 1 Quantum criticality above the upper critical dimension. The dispersion relation, dynamical exponent, effective dimension, $d_{\rm eff} = d + z$ and quantum critical exponent of the order parameter susceptibility χ in the self-consistent-field approximation to the quantum ϕ^4 field model for a displacive ferroelectric and for a metallic ferromagnet in three dimensions ($d = 3$). The self-consistent-field approximation is expected to be qualitatively correct for $d_{\rm eff} > 4$ and predicts $\chi \sim 1/T^{\gamma}$, where $\gamma = (d_{\rm eff} - 2)/z$ at the QCP. In the dispersion relation, κ is a correlation wavevector (proportional to Δ in the case of a ferroelectric QCP) that vanishes at the QCP. The fluctuation spectrum in the right-hand column is that expected for an itinerant-electron ferromagnet of interest here, which is characterized by a dynamical exponent of three. For comparison we note that at a magnetic QCP of an insulating magnet z is expected typically to be equal to two. An example of the applicability of a mean field model for a magnetic QCP of an insulating magnet with $z = 2$ has been given for a magnetic field induced QCP in $BaCuSi_2O_6$ [15, 16].

	ferroelectric[a] QCP	ferromagnetic QCP
fluctuation spectrum	$\omega_q^2 \sim \kappa^2 + q^2$	$\Gamma_q \sim q(\kappa^2 + q^2)$
$z(\kappa \to 0)$	1	3
$d_{\rm eff}$	4	6
χ	$1/T^2$	$1/T^{4/3}$

[a]Logarithmic correction to χ is expected since in this case $d_{\rm eff}$ is equal to the upper critical dimension.

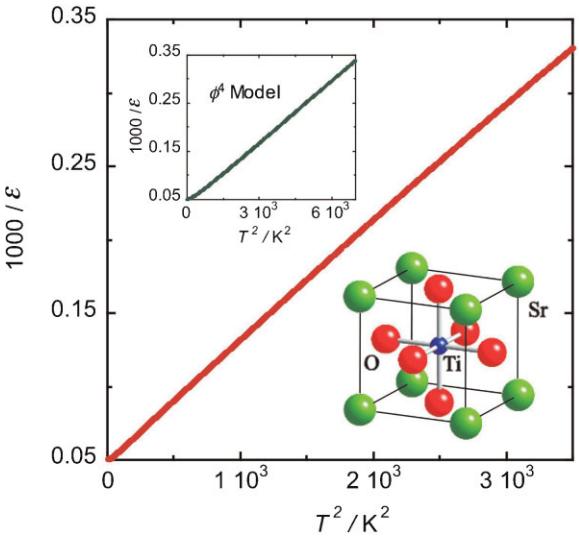

Figure 1 (online colour at: www.pss-b.com) Temperature dependence of the inverse dielectric function $\varepsilon = 1 + \chi$ near a ferroelectric QCP [12]. Comparison of the observed and predicted (inset) temperature dependence of $1/\varepsilon$ in $SrTiO_3$, a cubic perovskite on the border of a displacive ferroelectric transition at low temperatures (as discussed in the text, $d = 3$, $z = 1$). The observed quadratic temperature dependence of $1/\varepsilon$ is qualitatively consistent with the prediction of the self-consistent-field approximation of the quantum ϕ^4 field model, except at very low temperature as stated in the text. The zero temperature parameters of the model are estimated from the measured polarization vs. electric field equation of state as well as neutron scattering and Raman scattering experiments at low temperatures. The temperature dependence of ε is governed solely by the thermal factor in the model and the zero-temperature parameters. The cut-off wavevector in the calculation is taken to be the average radius of the Brillouin zone.

to 50 K just on the paraelectric side of a ferroelectric to paraelectric transition in the temperature-pressure phase diagram [12]. A similar behaviour has also been found in another paraelectric material somewhat further from the QCP, $KTaO_3$ [12]. The zero-temperature parameters of the model employed are obtained from measurements of the electric polarization versus electric field as well as from neutron and Raman scattering data. The temperature variation is given via a self-consistent solution of the ϕ^4 model, without the use of free adjustable parameters.

Shallow minima in the inverse dielectric functions observed at low temperatures in both materials are not, however, predicted by the above model. Potential mechanisms responsible for the observed minima include (i) the coupling between the critical optical mode and conventional acoustic modes [1, 13] and (ii) the long-range dipole–dipole interaction beyond the self-consistent field approximation [17], neither of which has been thus far taken into account in a quantitative fashion. Both of these effects can lead to an attractive interaction between fluctuation modes, *i.e.*, an attractive ϕ^4 term in the field model that can drastically change the susceptibility and other properties at very low temperatures. As we shall see below, the emergence of an attractive ϕ^4 term is of central importance also on the border of ferromagnetism.

3 Quantum tricriticality in an exchange enhanced paramagnet We next consider the corresponding problem of a quantum phase transition from a ferromagnetic to a paramagnetic state in a metal as a function of a quantum tuning parameter such as applied pressure. The corresponding self-consistent-field approximation to the quantum ϕ^4 field model in a metal is known as the self-consistent-renormalization (SCR) model, or equivalently the Moriya-Hertz-Millis model [3, 6, 18, 19], which has seen a number of independent and somewhat different developments. They have in common essentially a mean field decoupling of the interaction between field modes (*i.e.*, the Fourier components $\phi_q(\tau)$ of $\phi(r,\tau)$), but differ in some quantitative aspects (see, *e.g.*, discussions in Ref. [20]). In the calculations presented here we have employed the approach reviewed in Ref. [21].

In contrast to the paraelectrics, the spectrum of fluctuations of modes in the metallic state is governed by Landau damping together with the consequences of a vanishing inverse static magnetic susceptibility χ^{-1} as $T \to 0$ and $T_C \to 0$. This leads to a spin-fluctuation spectrum with imaginary frequency, $\Gamma_q \sim q^z$, where $z = 3$. The SCR model has been successful in accounting for a wide range of thermal and transport properties in d-electron metals with unsaturated spin polarizations and low T_C (see, *e.g.*, [18,

21]). However, near to and above the critical lattice density where $T_C \to 0$, the SCR model in its simplest form can break down. One of the mechanisms for the breakdown is the emergence (as in the ferroelectrics) of attractive interactions between critical fluctuation modes.

Consider, for example, the simple-cubic d-metal Ni_3Ga, which is a paramagnetic relative of the weakly ferromagnetic metal Ni_3Al (for recent discussions see Refs. [22, 23]). With a high Wilson ratio of over 30, Ni_3Ga is thought to be very close to the border of ferromagnetism at low temperatures. As can be inferred from Fig. 2 (and from the caption of Fig. 2), the temperature dependence of the inverse susceptibility is characterized by a temperature exponent of order two or higher instead of the predicted value of 4/3 (Table 1) [23].

This unexpected behaviour may perhaps be understood in terms of an extended form of the SCR model in which the mode-mode coupling ϕ^4 term is attractive and an additional positive stabilizing 'three-mode' coupling term of order ϕ^6 is included. This ϕ^6 SCR model leads to a temperature–pressure phase diagram that includes regions of first and second order transitions separated by a tricritical point (§5). The magnetic field and temperature dependence of the magnetic equation of state are consistent with this scenario and suggests that Ni_3Ga is on the border of a ferromagnetic tricritical point in the low temperature limit, *i.e.*, that it is on the border of essentially a quantum tricritical point that is dominated by the three-mode coupling term. The SCR model in this case predicts a leading $T^{8/3}$ rather than $T^{4/3}$ temperature dependence of χ^{-1}. As shown in the inset of Fig. 2 the ϕ^6 SCR model is indeed capable of describing the observed variation of χ^{-1} versus T at low temperatures [23]. The zero-temperature parameters of the model are obtained from the measured magnetic equation of state and inelastic neutron scattering data at low temperatures. The temperature dependence of χ^{-1} is then determined by the Bose-Einstein thermal factor in the model without the use of free adjustable parameters. The same general approach has been used in the case of the paraelectrics and essentially in the analyses given in the following section.

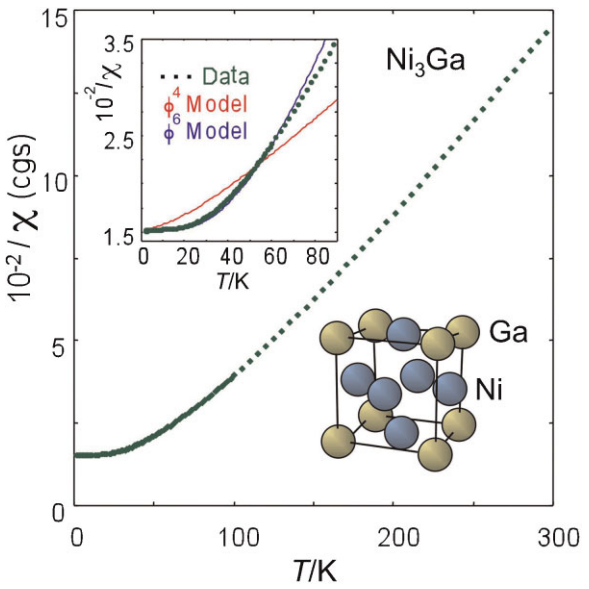

Figure 2 (online colour at: www.pss-b.com) Border of a quantum tricritical point [23]. The observed temperature dependence of the inverse of the magnetic susceptibility χ in the nearly ferromagnetic simple-cubic metal Ni_3Ga can be understood in terms of a ϕ^6 SCR model with an attractive ϕ^4 term and a repulsive ϕ^6 term ($d = z = 3$, inset). The zero temperature parameters of the model are estimated from the measured magnetic equation of state and neutron scattering data at low temperatures. The calculated temperature dependence of χ is governed by these zero-temperature parameters and the Bose-Einstein thermal factor. (For definitions of the ϕ^4 and ϕ^6 models referred to in the inset and for other details see Ref. [23].)

4 The non-local marginal Fermi liquid state in a weakly ferromagnetic metal We turn to the case of ferromagnetic d-electron metals with unsaturated spin polarization and low Curie temperatures. Between T_{FL} and T_{MFL} in the temperature–pressure phase diagram in Fig. 3, the SCR model with $d = 3$ reduces approximately to the non-local marginal Fermi liquid model [6, 18, 21, 25–27] characterized in particular by a $T^{5/3}$ temperature dependence of the electrical resistivity, ρ, and T-linear temperature dependence of the thermal resistivity, w, at low temperature. This is to be contrasted with the predictions of the local marginal Fermi liquid model [28] in which both ρ and w are linear in T at low temperatures.

The non-local marginal Fermi liquid has been discussed in other contexts [27] and for instance in cases where the relevant critical fields are (i) transverse gauge fields in

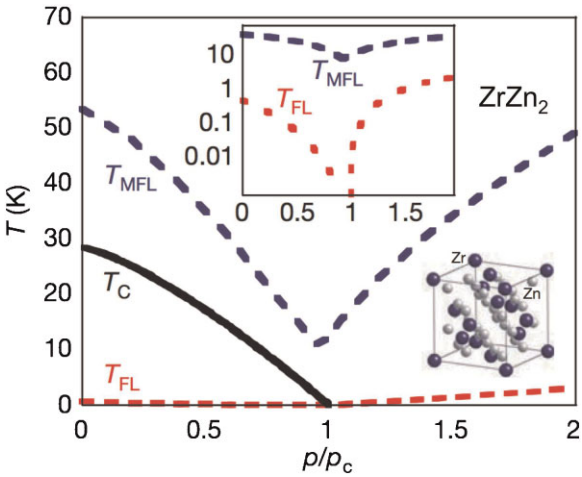

Figure 3 (online colour at: www.pss-b.com) Temperature–pressure phase diagram predicted by the SCR model for a weakly ferromagnetic metal, $ZrZn_2$ [24]. The solid line, labelled T_C, is the Curie temperature. Below the lower crossover line, T_{FL}, the SCR model predicts Fermi liquid behaviour characterized by a T^2 resistivity. Above T_{FL} up to T_{MFL} (excluding a narrow regime near T_C), the SCR model predicts non-local marginal Fermi liquid behaviour characterized by a $T^{5/3}$ electrical resistivity and T-linear thermal resistivity ($d = z = 3$).

ideally pure metals [25, 26] or (ii) statistical gauge fields on the border of electron localization [29]. In these and other related examples (see *e.g.*, [30]) the dynamical exponent is also three and the temperature dependence of, *e.g.*, the heat capacity is predicted to be of the same form as that of the SCR model for a ferromagnetic QCP.

We consider the example of $ZrZn_2$ that crystallizes in a cubic laves structure (Fig. 3) (see Refs. [24, 31–34] for recent discussions). As shown in Fig. 4, the observed temperature dependences of ρ and w are consistent with the predictions of the SCR model [24]. The correspondence between theory and experiment suggests that the temperature variations of ρ and w at low T are governed mainly by the effects of scattering of carriers from nearly critical ferromagnetic spin fluctuations. Scattering from phonons is found to be subdominant below about 15 K in both ρ and w for samples having residual resistivities well below 1 μΩ cm [24, Supplementary Information].

The $T^{5/3}$ temperature dependence of ρ is observed to extend up to the critical pressure p_c of approximately 20 kbar where $T_C \to 0$ in $ZrZn_2$ (Fig. 5). However, the temperature dependence changes abruptly from $T^{5/3}$ to $T^{3/2}$ upon crossing p_c, a result inconsistent with the predictions of the SCR model in its conventional form (inset of Fig. 5) [24, 34]. The $T^{3/2}$ resistivity extends from p_c up to at least twice p_c [34, 35]. Intriguingly, similar behaviour, suggestive of the existence of a critical regime rather than a critical point, has been reported in other materials on the border of magnetic phase transitions and in particular in MnSi [36–38] and $YbAlB_4$ [39].

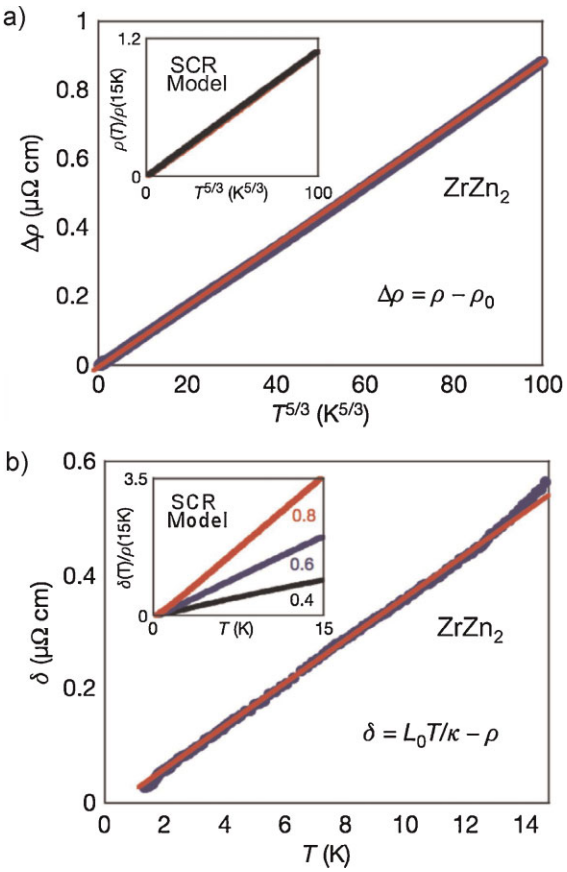

Figure 4 (online colour at: www.pss-b.com) Temperature dependence of transport properties in a weakly ferromagnetic metal, $ZrZn_2$ [24]. (a) The temperature dependence of the electrical resistivity, ρ, and (b) the temperature dependence of the difference δ between the thermal resistivity w and ρ, where $w = L_0T/\kappa$, κ is the thermal conductivity and L_0 is the Lorentz number. The $T^{5/3}$ electrical resistivity and T-linear thermal resistivities are consistent with the predictions of the SCR model ($d = z = 3$, insets in (a) and (b)) [18]. The zero temperature model parameters were obtained in a manner similar to that described in the caption of Fig. 3. The cut-off wavevector in the model is taken to be the average radius of the Brillouin zone, and the values given in the inset of (b) correspond to possible characteristic dimensions (in inverse Angstrom) of the relevant Fermi surface sheet. In the pure samples used here with residual resistivities of 0.2 μΩ cm the effect of phonons on w is found to be small and ignorable below approximately 15 K.

5 Magnetic inhomogeneities above p_c Both $ZrZn_2$ [40] and MnSi [41] exhibit weak first order transitions just below p_c and may be described, as in the case of Ni_3Ga and other ferromagnetic metals, by a temperature–pressure-magnetic field phase diagram of the form shown schematically in Fig. 6 [37, 42]. In this figure a second order transition line falls with increasing pressure and bifurcates at a tricritical point leading to two sheets of first order transitions (the negative magnetic field sheet is not shown).

The state near to the tricritical point in materials such as MnSi is characterized by slowly varying magnetic inhomogeneities not described by the SCR model in its current form

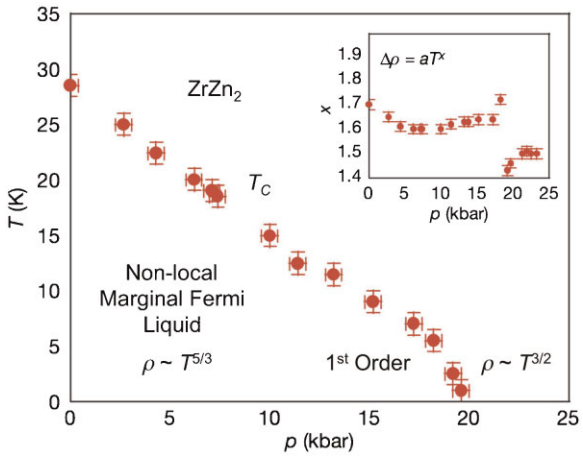

Figure 5 (online colour at: www.pss-b.com) Temperature–pressure phase diagram of $ZrZn_2$ [24]. The magnetic transition becomes weakly first order near to the critical pressure p_c of the order of 20 kbar [40]. The resistivity varies as $T^{5/3}$ below p_c and as $T^{3/2}$ above p_c (upper inset) (see also Refs. [32, 34]). The $T^{3/2}$ resistivity, found to extend from p_c to at least twice p_c within the temperature range 1 to 15 K [34, 35], is inconsistent with the predictions of the SCR model in its conventional form.

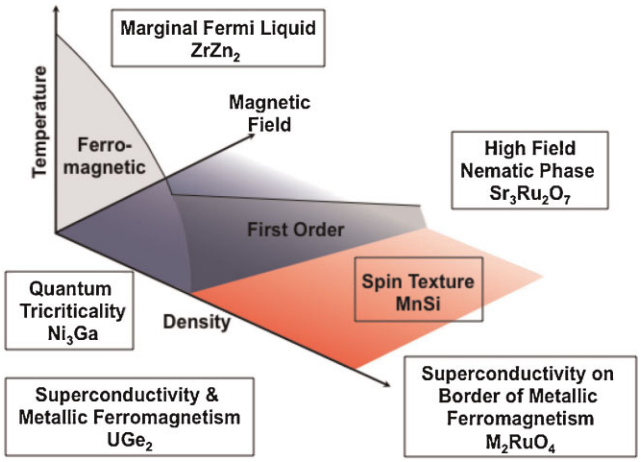

Figure 6 (online colour at: www.pss-b.com) Temperature–pressure–magnetic field phase diagram on the border of ferromagnetism. Qualitative form of the phase diagram predicted by the ϕ^6 SCR model with an attractive ϕ^4 term in the effective action [36, 37, 42]. Selected examples of phenomena observed on the border of ferromagnetism are also listed. Besides the cases discussed in the text we have also included (i) an example of the coexistence of superconductivity and metallic ferromagnetism (UGe_2 [59–61]), (ii) spin-triplet superconductivity on the border of ferromagnetism (M_2RuO_4, where M stands for Sr [62, 63] or potentially Ca at high pressures) and (iii) an electronic nematic phase in $Sr_3Ru_2O_7$ [64, 65] near to a quantum critical end point in high magnetic fields.

[43–45]. The existence of a tricritical point and magnetic inhomogeneities near to and above p_c has been attributed, for example, to (i) the magneto-elastic coupling [46], (ii) anharmonic quantum precession of the magnetization [18, 21, 47] and (iii) non-analytic corrections to the magnetic equation of state expected to arise when full account is taken of the effects of gapless particle-hole excitations at the Fermi surface [48–53]. These effects lead to attractive interactions between spin fluctuation modes and to a phase diagram of the form shown in Fig. 6. Potentially they also lead to intrinsic magnetic inhomogeneities near to p_c.

In principle, first order transitions and inhomogeneities can also arise via the effects of van Hove and nesting singularities of the Fermi surface [18, 54–57]. A Fermi surface such as that predicted for paramagnetic $ZrZn_2$, that is characterized both by a low Fermi velocity at k-points near to van Hove singularities along <111> directions and strong nesting along <100> directions, would be consistent with the existence of enhanced ferromagnetic as well as antiferromagnetic spin fluctuations [56, 57]. This could lead to the existence of two quasi-critical fields and to a state that is more inhomogeneous than expected in the presence of ferromagnetic fluctuations alone. We also note that such a Fermi surface model can lead to a first order transition to ferromagnetism at sufficiently small lattice density and to a phase diagram of the form shown in Fig. 6 [54–57]. A more recent example in which these effects may be important is reported in Ref. [58] and these proceedings.

6 Additional phase transitions A study of the simplest d-electron metals reveals that the border of ferromagnetism appears to be characterized by a multiplicity of quasi-critical fields and potentially a multiplicity of phase transitions (Fig. 6). The border of ferromagnetism, and also of ferroelectricity as suggested at the end of §2, can thus be more intriguing than was generally envisaged in the early work on quantum critical phenomena. The occurrence of a multiplicity of quantum critical fields is not limited to the problems that we have considered but appears to be a recurrent theme in the study of quantum phase transitions in general.

For instance, the case of high T_c cuprates is thought to involve a plethora of neighbouring phases, including antiferromagnetism, electron nematic order, d-wave superconductivity and perhaps multiple quantum liquid states on

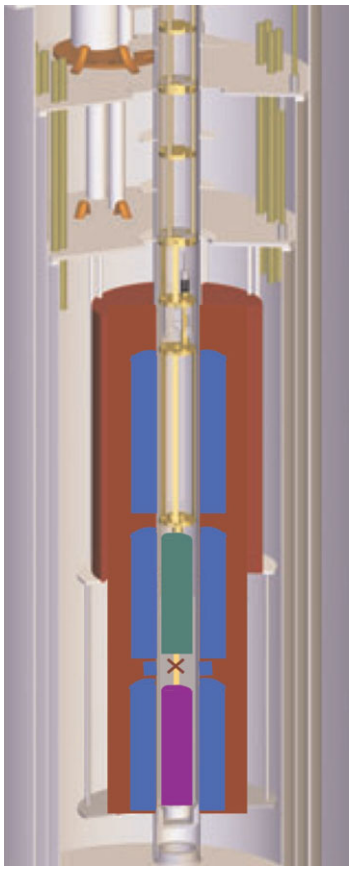

Figure 7 (online colour at: www.pss-b.com) Surveying quantum phase transitions. Cryogen-free automated system for scanning over wide ranges in temperature, magnetic field and pressure. The figure illustrates the cryomagnetic system being developed in a collaboration between Dryogenics Ltd and the Cavendish Laboratory for routine scans from room temperature to the low millikelvin range employing a pulse tube cryocooler (40 K and 4 K plates on top) and a two-stage magnetic refrigerator (two magnets and two pills at bottom). The experimental region (with surrounding magnet in middle) accommodates a variable-pressure diamond-anvil cell designed for electronic and magnetic measurements under quasi-hydrostatic conditions.

the border of Mott transitions. The f-electron heavy-fermion systems can also exhibit analogous remarkable phenomena on the edge of f-electron localization. A number of systems on the border of electron localization are discussed in this volume. The diverse views reported on the nature of f-electron heavy fermion systems related in part to the magnetic metals discussed here can be inferred for example from Refs. [29–30, 66–77]. The f-electron systems display not only a multiplicity of quantum critical fields, but also show evidence of scaling behaviours not expected in terms of the early models of quantum critical phenomena (see, *e.g.*, [78–80]).

Detailed examinations of quantum phase transitions require scans of broad regions of phase space by the precise and painstaking control of tuning parameters including temperature, pressure, magnetic field, electric field and materials properties. A recent example of the utility of such phase space exploration in uncovering unconventional phenomena is provided by the observation in $SrFe_2As_2$ and $BaFe_2As_2$ of pressure-induced superconductivity with T_c of up to $\sim$30 K (the highest reported, up to the time of discovery, in any material not superconducting at ambient pressure) [81]. An automated cryogen-free measurement system that may help to facilitate studies of quantum phase transitions and the search for novel phenomena in the future is illustrated in our concluding figure (Fig. 7). This system, which is currently under development, allows the temperature to be changed between room temperature and the low millikelvin range with built-in pressure and magnetic field control technology. This allows the option of varying the pressure *in situ* with a diamond anvil cell at low temperatures.

Acknowledgements We are grateful for discussions with P. Chandra, P. Coleman, G. J. Conduit, F. M. Grosche, R. K. W. Haselwimmer, D. E. Khmelnitskii, P. Littlewood, A. P. Mackenzie, P. Monthoux, J. F. Scott, L. Sibley, B. D. Simon, D. Tompsett, I. R. Walker and J. Wensley. We also thank S. V. Brown, G. L. Lonzarich and D. Astill for their invaluable assistance. The Engineering and Physical Sciences Research Council of the United Kingdom, the Royal Society of London, the Isaac Newton Trust, and Jesus, Emmanuel and Trinity Colleges have supported this work.

References

[1] D. E. Khmelnitskii and V. L. Shneerson, Sov. Phys. – Solid State **13**, 687 (1971); Sov. Phys. JETP **37**, 164 (1973).
[2] K. K. Murata and S. Doniach, Phys. Rev. Lett. **29**, 285 (1972).
[3] T. Moriya and A. Kawabata, J. Phys. Soc. Jpn. **34**, 639 (1973); J. Phys. Soc. Jpn. **35**, 669 (1973).
[4] T. V. Ramakrishnan, Phys. Rev. B **10**, 4014 (1974).
[5] I. E. Dzyaloshinskii and P. S. Kondratenko, Sov. Phys. JETP **43**, 1036 (1976).
[6] J. A. Hertz, Phys. Rev. B **14**, 1165 (1976).
[7] S. Sachdev, Quantum Phase Transitions (Cambridge University Press, Cambridge, 1999).
[8] P. W. Anderson, Phys. B **318**, 28 (2002).
[9] R. B. Laughlin, G. G. Lonzarich, P. Monthoux, and D. Pines, Adv. Phys. **50**, 361 (2001).
[10] K. A. Müller and H. Burkard, Phys. Rev. B **19**, 3593 (1979).
[11] R. Roussev and A. J. Millis, Phys. Rev. B **67**, 014105 (2003).
[12] S. E. Rowley, L. J. Spalek, R. P. Smith, M. P. M. Dean, G. G. Lonzarich, J. F. Scott, and S. S. Saxena, arXiv:0903.1445 [cond-mat.str-el] (2009).
[13] L. Pálová, P. Chandra, and P. Coleman, Phys. Rev. B **79**, 075101 (2009).
[14] N. Das and S. G. Mishra, J. Phys.: Condens. Matter **21**, 095901 (2009).
[15] S. E. Sebastian, N. Harrison, C. D. Batista, L. Balicas, M. Jaime, P. A. Sharma, N. Kawashima, and I. R. Fisher, Nature **441**, 617 (2006).
[16] C. D. Batista, J. Schmalian, N. Kawashima, P. Sengupta, S. E. Sebastian, N. Harrison, M. Jaime, and I. R. Fisher, Phys. Rev. Lett. **98**, 257201 (2007).
[17] G. J. Conduit and B. D. Simons, arXiv: 0909.5660v1 [cond-mat.str-el] (2009).
[18] T. Moriya, Spin Fluctuations in Itinerant Electron Magnetism (Springer, Berlin, 1985).
[19] A. J. Millis, Phys. Rev. B **48**, 7183 (1993).
[20] G. G. Lonzarich and L. Taillefer, J. Phys. C: Solid State Phys. **18**, 4339 (1985).
G. G. Lonzarich, J. Magn. Magn. Mater. **54–57**, 612 (1986).
[21] G. G. Lonzarich, The Magnetic Electron, Electron (Cambridge University Press, Cambridge, 1997).
[22] P. G. Niklowitz, F. Beckers, and G. G. Lonzarich, Phys. Rev. B **72**, 024424 (2005).
[23] R. P. Smith, J. Phys.: Condens. Matter **21**, 095601 (2009).
[24] R. P. Smith, M. Sutherland, G. G. Lonzarich, S. S. Saxena, N. Kimura, S. Takashima, M. Nohara, and H. Takagi, Nature **455**, 1220 (2008).
[25] T. Holstein, R. E. Norton, and P. Pincus, Phys. Rev. B **8**, 2649 (1973).
[26] M. Yu. Reizer, Phys. Rev. B **39**, 1602 (1989).
[27] G. Baym and C. Pethick, Landau Fermi Liquid Theory: Concepts and Applications (Wiley, New York, 1991), Ch. 3.
[28] C. M. Varma, P. B. Littlewood, S. Schmitt-Rink, E. Abrahams, and A. E. Ruckenstein, Phys. Rev. Lett. **63**, 1996 (1989).
[29] T. Senthil, M. Vojta, and S. Sachdev, Phys. Rev. B **69**, 035111 (2004).
[30] I. Paul, C. Pépin, and M. R. Norman, Phys. Rev. Lett. **98**, 026402 (2007).
[31] S. J. C. Yates, G. Santi, S. M. Hayden, P. J. Meeson, and S. B. Dugdale, Phys. Rev. Lett. **90**, 057003 (2003).
[32] E. A. Yelland, S. J. C. Yates, O. Taylor, A. Griffiths, S. M. Hayden, and A. Carrington, Phys. Rev. B **72**, 184436 (2005).
[33] D. A. Sokolov, M. C. Aronson, W. Gannon, and Z. Fisk, Phys. Rev. Lett. **96**, 116404 (2006).
[34] S. Takashima, M. Nohara, H. Ueda, N. Takashita, C. Terakura, F. Sakai, and H. Takagi, J. Phys. Soc. Jpn **76**, 043704 (2007).
[35] L. Sibley and J. Wensley, private communications.
[36] C. Pfleiderer, S. R. Julian, and G. G. Lonzarich, Nature **414**, 427 (2001).
[37] N. Doiron-Leyraud, I. R. Walker, L. Taillefer, M. J. Steiner, S. R. Julian, and G. G. Lonzarich, Nature **425**, 595 (2003).
[38] P. Pedrazzini, D. Jaccard, G. Lapertot, J. Flouquet, Y. Inada, H. Kohara, and Y. Onuki, Physica B **378–380**, 165 (2006).
[39] S. Nakatsuji et al., Nature Phys. **4**, 603 (2008).
[40] M. Uhlarz, C. Pfleiderer, and S. M. Hayden, Phys. Rev. Lett. **93**, 256404 (2004).

[41] C. Pfleiderer, G. J. McMullan, S. R. Julian, and G. G. Lonzarich, Phys. Rev. B **55**, 8330 (1997).
[42] D. Belitz, T. R. Kirkpatrick, and J. Roolbühler, Phys. Rev. Lett. **94**, 247205 (2005).
[43] W. Yu, F. Zamborsky, D. Thompson, J. L. Sarrao, M. E. Torelli, Z. Fisk, and S. E. Brown, Phys. Rev. Lett. **92**, 086403 (2004).
[44] C. Pfleiderer, D. Reznik, L. Pintschovius, H. v. Löhneysen, M. Garst, and A. Rosch, Nature **427**, 227 (2004).
[45] Y. J. Uemura et al., Nature Phys. **3**, 29 (2006).
[46] G. A. Gehring, Europhys. Lett. **82**, 60004 (2008).
[47] M. T. Béal-Monod, S.-K. Ma, and D. R. Fredkin, Phys. Rev. Lett. **20**, 929 (1968).
[48] S. Misawa, Phys. Rev. Lett. **26**, 1632 (1971).
[49] G. Barnea and D. M. Edwards, J. Phys. F, Metal Phys. **7**, 1323 (1977).
[50] D. Belitz, T. R. Kirkpatrick, and T. Vojta, Phys. Rev. B **55**, 9452 (1997).
[51] G. Y. Chitov and A. J. Millis, Phys. Rev. B **86**, 5337 (2001).
[52] A. V. Chubukov and D. L. Maslov, Phys. Rev. B **69**, 121102 (2004).
[53] G. J. Conduit, A. G. Green, and B. D. Simons, arXiv: 0906.1347v1 [cond-mat.str-el] (2009).
[54] J. Kübler, Phys. Rev. B **70**, 064427 (2004).
[55] I. I. Mazin and D. J. Singh, Phys. Rev. B **69**, 020402 (2004).
[56] T. Jeong, A. Kyker, and W. E. Pickett, Phys. Rev. B **73**, 115106 (2006).
[57] D. Tompsett, private communications 2009.
[58] M. Brando, W. J. Duncan, D. Moroni-Klementowicz, C. Albrecht, D. Grüner, R. Ballou, and F. M. Grosche, Phys. Rev. Lett. **101**, 026401 (2008).
[59] S. S. Saxena et al., Nature **406**, 587 (2000).
[60] A. Harada, S. Kawasaki, H. Mukuda, Y. Kitaoka, Y. Haga, E. Yamamoto, Y. Onuki, K. M. Ktoh, E. E. Haller, and H. Harima, Phys. Rev. B **75**, 140502 (2007).
[61] A. D. Huxley, S. J. C. Yates, F. Levy, and I. Sheikin, J. Phys. Soc. Jpn. **76**, 051011 (2007).
[62] Y. Maeno et al., Nature **372**, 532 (1994).
[63] A. P. Mackenzie and Y. Maeno, Rev. Mod. Phys. **75**, 657 (2003).
[64] S. A. Grigera, R. S. Perry, A. J. Schofield, M. Chiao, S. R. Julian, G. G. Lonzarich, S. I. Ikeda, Y. Maeno, A. J. Millis, and A. P. Mackenzie, Science **294**, 329 (2001).
[65] R. A. Borzi, S. A. Grigera, J. Farrell, R. S. Perry, S. J. S. Lister, S. L. Lee, D. A. Tennant, Y. Maeno, and A. P. Mackenzie, Science **315**, 214 (2007).
[66] P. Thalmeier, G. Zwicknagl, O. Stockert, G. Spain, and F. Steglich, Frontiers in Superconducting Materials (Springer, Berlin, 2004), pp 769–787.
[67] Y. Onuki et al., J. Phys. Soc. Jpn **73**, 769 (2004).
[68] P. Coleman and A. J. Schofield, Nature **433**, 226 (2005).
[69] A. J. Schofield, Phys. World **16**, 23 (2003).
[70] M. B. Maple, N. A. Frederick, P.-C. Ho, W. M. Yuhasz, and T. Yanagisawa, J. Supercond. Novel Magn. **19**, 299 (2006).
[71] G. R. Stewart, Mod. Phys. **73**, 797 (2001); Mod. Phys. **78**, 743 (2006).
[72] P. Gegenwart, T. Westerkamp, C. Krellner, Y. Tokiwa, S. Paschen, C. Geibel, F. Steglich, E. Abrahams, and Q. Si, Science **315**, 969 (2007).
[73] H. v. Löhneysen, A. Rosch, M. Vojta, and P. Wölfle, Rev. Mod. Phys. **79**, 1015 (2007).
[74] P. Monthoux, D. Pines, and G. G. Lonzarich, Nature **450**, 1177 (2007).
[75] Y.-F. Yang, Z. Fisk, H.-O. Lee, J. D. Thompson, and D. Pines, Nature **454**, 611 (2008).
[76] J. Flouquet and H. Harima, arXiv:0910.3110 [cond-mat. str-el] (2009).
[77] S. Friedemann, T. Westerkamp, M. Brando, N. Oeschler, S. Wirth, P. Gegenwart, C. Krellner, C. Geibel, and F. Steglich, Nature Phys. **5**, 465 (2009).
[78] M. C. Aronson et al., Phys. Rev. Lett. **75**, 725 (1995).
[79] A. Schröder et al., Nature **407**, 351 (2000).
[80] Q. Si, S. Rabello, K. Ingersent, and J. L. Smith, Nature **413**, 804 (2001).
[81] P. L. Alireza, Y. T. C. Ko, J. Gillett, C. M. Petrone, J. M. Cole, G. G. Lonzarich, and S. E. Sebastian, J. Phys.: Condens. Matter **21**, 012208 (2009).